東北大学機関リポジトリ
TOUR
Tohoku University Repository

Theoretical studies of a simulcast digital radio paging system using a carrier frequency offset strategy

著者	安達　文幸
journal or publication title	IEEE Transactions on Vehicular Technology
volume	29
number	1
page range	87-95
year	1980
URL	http://hdl.handle.net/10097/46504

Theoretical Studies of a Simulcast Digital Radio Paging System Using a Carrier Frequency Offset Strategy

TAKESHI HATTORI, MEMBER, IEEE, KENKICHI HIRADE, MEMBER, IEEE, AND FUMIYUKI ADACHI, MEMBER, IEEE

Abstract—**In a multistation simulcast digital radio paging system, each base station transmits the same RF signal simultaneously with the resulting efficient frequency utilization and simplified receiver design. In this system a paging receiver in the overlapping area receives several RF signals transmitted from different base stations. When frequency-shift keying (FSK) is used as a modulation method, experimental test results have already shown that the timing of each RF signal should be synchronized as closely as possible, but that the carrier frequency of each transmitter should be set following a certain offset assignment. The signal transmission performance in a multipath fading environment can then be markedly improved. The cause of this improvement effect is theoretically analyzed. It is clarified that the improvement effect is caused by transforming the probability distribution of time-averaged signal power.**

I. INTRODUCTION

MANY mobile telephone and personal paging systems require signaling simultaneously from multiple transmitters. This type of signaling is often termed the simulcasting technique, in which the same baseband information is simultaneously broadcast over a multistation transmitter system operating on a single nominal-carrier frequency. Many simulcasting techniques concerning the analog voice transmission have been proposed and introduced in the actual systems [1]. Recently, radio paging systems using digital signal transmission techniques are also being studied in order to obtain increased capacity, receiver miniaturization, improved grade of service, and so on [2], [3]. In this case the whole service area is generally divided into many subareas, i.e., radio zones having an individual transmitting base station due to restrictions in transmitting power and antenna gain. In such a radio paging system, it is desirable for each base station to transmit the same RF signal simultaneously in order to obtain efficient frequency utilization and simplified receiver construction. A paging receiver in the overlapping area of such a simulcast system receives several RF signals transmitted from different base stations.

It might be intuitively understood that the timing of each RF signal being transmitted and the carrier frequency of each transmitter should be closely synchronized in the whole service area. In case of FSK being used as the modulation method, experimental test results have already shown that the timing of each RF signal should be synchronized as closely as possible, but the carrier frequency of each transmitter should be set following a given offset assignment [2], [3]. When the center frequencies are set under an optimum offset assignment, the signal transmission performance in the multipath fading environment can be markedly improved. The cause of its improvement effect has never been theoretically analyzed. This paper gives a theoretical analysis of its improvement effect.

Manuscript received October 14, 1978; revised August 27, 1979.

The authors are with the Yokosuka Electrical Communication Laboratory, Nippon Telegraph and Telephone Public Corp., 1-2356, Take, Yokosuka-shi, Kanagawa-ken, 238-03, Japan.

II. MATHEMATICAL REPRESENTATION OF COMBINED SIGNAL

Let us consider that a person with a paging receiver is moving at a constant speed in the overlapping area between two adjacent zones, and that binary frequency-shift keying (FSK) signals modulated by the same baseband pulse $m(t)$ are simultaneously transmitted from two base stations located far away. Although both FSK signals have identical frequency deviation $\pm\Delta f_d$, their center frequencies f_1 and f_2 are not synchronized but are set under a certain offset assignment. These FSK signals are combined and received by the paging receiver. Therefore, the system model is as shown by the block diagram in Fig. 1.

As the signal transmission from each base station to the paging receiver generally follows multiple random paths, multipath fading phenomenon occurs on each of the received FSK signals. Such a multipath fading phenomenon can be represented by a narrow-band Gaussian process having a Rayleigh distributed envelope and a uniformly distributed phase [4]. Considering that the transmission paths from each base station to the paging receiver are different from each other, the multipath fading phenomena associated with the received FSK signals are mutually independent. Therefore, the received FSK signals $e_1(t)$ and $e_2(t)$ are given by

$$\begin{aligned} e_1(t) &= x_1(t)\cos\left\{2\pi f_1 t + 2\pi\Delta f_d \int_{-\infty}^{t} m(\xi)\,d\xi\right\} \\ &\quad - y_1(t)\sin\left\{2\pi f_1 t + 2\pi\Delta f_d \int_{-\infty}^{t} m(\xi)\,d\xi\right\} \\ e_2(t) &= x_2(t)\cos\left\{2\pi f_2 t + 2\pi\Delta f_d \int_{-\infty}^{t} m(\xi)\,d\xi\right\} \\ &\quad - y_2(t)\sin\left\{2\pi f_2 t + 2\pi\Delta f_d \int_{-\infty}^{t} m(\xi)\,d\xi\right\} \end{aligned} \tag{1}$$

where the baseband modulation pulse $m(t)$ with repetition period T_b is given by

$$m(t) = \sum_{n=-\infty}^{\infty} a_n g(t - nT_b) \tag{2}$$

0018-9545/80/0200-0087$00.75 © 1980 IEEE

Authorized licensed use limited to: TOHOKU UNIVERSITY. Downloaded on March 07,2010 at 19:56:16 EST from IEEE Xplore. Restrictions apply.

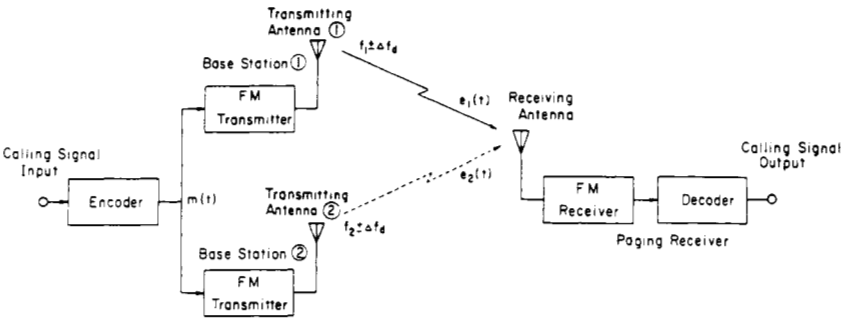

Fig. 1. Block diagram of digital radio paging system.

where

$$a_n = \begin{cases} +1, & \text{for mark} \\ -1, & \text{for space} \end{cases}$$

$$g(t) = \begin{cases} 1, & t \epsilon [-T_b/2, T_b/2] \\ 0, & \text{elsewhere} \end{cases}$$

and $x_i(t)$ and $y_i(t)$ $(i = 1, 2)$ are mutually independent stationary zero-mean baseband Gaussian processes satisfying the following relations:

$$\begin{aligned} &\langle x_1(t)\rangle_{\text{av}} = \langle y_1(t)\rangle_{\text{av}} = \langle x_2(t)\rangle_{\text{av}} = \langle y_2(t)\rangle_{\text{av}} = 0 \\ &\langle x_1(t)x_1(t \pm \tau)\rangle_{\text{av}} = \langle y_1(t)y_1(t \pm \tau)\rangle_{\text{av}} = \sigma_1{}^2\varphi_1(\tau) \\ &\langle x_2(t)x_2(t \pm \tau)\rangle_{\text{av}} = \langle y_2(t)y_2(t \pm \tau)\rangle_{\text{av}} = \sigma_2{}^2\varphi_2(\tau) \\ &\langle x_1(t)y_1(t \pm \tau)\rangle_{\text{av}} = \langle x_1(t)y_2(t \pm \tau)\rangle_{\text{av}} \\ &\qquad = \langle x_1(t)x_2(t \pm \tau)\rangle_{\text{av}} = 0 \\ &\langle x_2(t)y_1(t \pm \tau)\rangle_{\text{av}} = \langle x_2(t)y_2(t \pm \tau)\rangle_{\text{av}} \\ &\qquad = \langle y_1(t)y_2(t \pm \tau)\rangle_{\text{av}} = 0 \end{aligned} \tag{3}$$

where $\langle \cdot \rangle_{\text{av}}$ denotes the statistical average. Furthermore, σ_i^2 is the average power of $e_i(t)$ and $\varphi_i(\tau)$ is the autocorrelation function of $x_i(t)$ and $y_i(t)$. Assuming for an example that an antenna having an omnidirectional pattern in the horizontal plane is used as the receiving antenna and that the vertically polarized parts of the incident waves are uniformly distributed with respect to azimuth angle, $\varphi_i(\tau)$ is given by [4]

$$\varphi_1(\tau) = \varphi_2(\tau) = J_0(2\pi f_D \mid \tau \mid) \tag{4}$$

where $J_0(\cdot)$ denotes the zeroth order Bessel function of the first kind and f_D is the maximum Doppler shift frequency given by the following relation at movement speed v and carrier wavelength λ:

$$f_D = v/\lambda. \tag{5}$$

Because the FSK signals $e_1(t)$ and $e_2(t)$ are combined at the receiving antenna, the total input signal $e(t)$ received by the paging receiver is given by

$$e(t) = e_1(t) + e_2(t). \tag{6}$$

Substituting (1) into (6), the combined input signal $e(t)$ can be represented as

$$\begin{aligned} e(t) = {} & x(t) \cos \left\{ 2\pi f_c t + 2\pi \Delta f_d \int_{-\infty}^{t} m(\xi)\, d\xi \right\} \\ & - y(t) \sin \left\{ 2\pi f_c t + 2\pi \Delta f_d \int_{-\infty}^{t} m(\xi)\, d\xi \right\} \end{aligned} \tag{7}$$

where f_c is the equivalent center frequency given by

$$f_c = (\sigma_1{}^2 f_1 + \sigma_2{}^2 f_2)/(\sigma_1{}^2 + \sigma_2{}^2). \tag{8}$$

Furthermore, $x(t)$ and $y(t)$ are given by

$$\begin{aligned} x(t) = {} & x_1(t) \cos (2\pi \Delta f_1 t) - y_1(t) \sin (2\pi \Delta f_1 t) \\ & + x_2(t) \cos (2\pi \Delta f_2 t) - y_2(t) \sin (2\pi \Delta f_2 t) \\ y(t) = {} & -x_1(t) \sin (2\pi \Delta f_1 t) + y_1(t) \cos (2\pi \Delta f_1 t) \\ & - x_2(t) \sin (2\pi \Delta f_2 t) + y_2(t) \cos (2\pi \Delta f_2 t) \end{aligned} \tag{9}$$

where Δf_1 and Δf_2 denote the equivalent offset frequencies given by

$$\begin{aligned} \Delta f_1 &= f_1 - f_c \\ \Delta f_2 &= f_2 - f_c. \end{aligned} \tag{10}$$

Assuming that the center frequencies f_1 and f_2 of the two FSK signals are set under the following offset assignment condition:

$$f_1 - f_2 = \Delta f \tag{11}$$

equivalent offset frequencies f_1 and f_2 are given by

$$\begin{aligned} \Delta f_1 &= (\sigma_2{}^2 \Delta f)/(\sigma_1{}^2 + \sigma_2{}^2) \\ \Delta f_2 &= -(\sigma_1{}^2 \Delta f)/(\sigma_1{}^2 + \sigma_2{}^2). \end{aligned} \tag{12}$$

As $x_i(t)$ and $y_i(t)$ $(i = 1, 2)$ are four stationary independent

Authorized licensed use limited to: TOHOKU UNIVERSITY. Downloaded on March 07,2010 at 19:56:16 EST from IEEE Xplore. Restrictions apply.

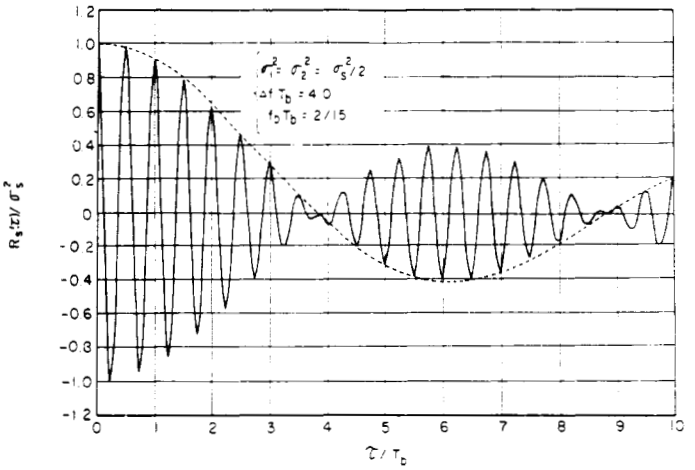

Fig. 2. Covariance function of combined signal.

zero-mean baseband Gaussian processes satisfying (3), $x(t)$ and $y(t)$ become mutually independent stationary zero-mean baseband Gaussian processes satisfying the following relations:

$$\begin{aligned} &\langle x(t)\rangle_{\mathrm{av}} = \langle y(t)\rangle_{\mathrm{av}} = 0 \\ &\langle x(t)x(t \pm \tau)\rangle_{\mathrm{av}} = \langle y(t)y(t \pm \tau)\rangle_{\mathrm{av}} = R_s(\tau) \\ &\langle x(t)y(t \pm \tau)\rangle_{\mathrm{av}} = 0 \end{aligned} \tag{13}$$

where $R_s(\tau)$ is the covariance function of $x(t)$ and $y(t)$ given by

$$\begin{aligned} R_s(\tau) = \{&\sigma_1{}^2 \cos(2\pi\Delta f_1\tau) \\ &+ \sigma_2{}^2 \cos(2\pi\Delta f_2\tau)\}J_0(2\pi f_D \mid \tau \mid). \end{aligned} \tag{14}$$

Therefore, the combined signal $e(t)$ can also be represented as a narrow-band Gaussian process having a Rayleigh distributed envelope and a uniformly distributed phase. Comparing (13) with (3), it is obvious that there exists only the difference between their covariance functions. Letting τ be zero in (14), the following relation exists:

$$R_s(0) = \sigma_s{}^2 = \sigma_1{}^2 + \sigma_2{}^2 \tag{15}$$

where σ_s^2 denotes the average signal power of the combined input signal. This means that the average power of $e(t)$ is given by the sum of the average power of $e_1(t)$ and $e_2(t)$. Furthermore, it is confirmed that (13) is equal to (3) by reducing σ_1^2 or σ_2^2 to zero in (14). This means that the combined signal becomes one of the received signals when either of the received average power values is extremely small. The covariance function of the combined signal is shown in Fig. 2.

III. RECEIVER MODEL

After being contaminated by additive thermal noise $n(t)$, the combined signal $e(t)$ is detected by the paging receiver shown in Fig. 3. The paging receiver, using an energy detection scheme, is composed of a pair of bandpass filters with a square-law envelope detector, a baseband difference circuit, and an integrate-dump circuit. In this receiver, which signal is transmitted is decided in accordance with the following quantity

$$I = \frac{1}{T_b} \int_{-T_b/2}^{T_b/2} \{v_m(t) - v_s(t)\}\, dt \tag{16}$$

being positive or negative. In (16) $v_m(t)$ and $v_s(t)$ denote baseband outputs of the square-law envelope detectors. The center frequencies f_m and f_s of the bandpass filters are set equal to the mark and space frequencies given by

$$\begin{aligned} f_m &= f_c + \Delta f_d \\ f_s &= f_c - \Delta f_d. \end{aligned} \tag{17}$$

Furthermore, considering that the power spectra of the received signals are given as shown in Fig. 4, the bandwidth B of each bandpass filter is set as

$$B = 2f_b + \Delta f \tag{18}$$

in order to pass the combined signal without distortion. In (18) $f_b = 1/T_b$ denotes the signaling frequency.

In the above-mentioned receiver model the additive thermal noise $n(t)$ is a stationary zero-mean white Gaussian noise with a uniformly distributed power density N_0. Then, both bandpass filtered noises $n_m(t)$ and $n_s(t)$ can be represented as stationary zero-mean narrow-band Gaussian processes given by

$$\begin{aligned} n_m(t) &= n_m{}^c(t)\cos(2\pi f_m t) - n_m{}^s(t)\sin(2\pi f_m t) \\ n_s(t) &= n_s{}^c(t)\cos(2\pi f_s t) - n_s{}^s(t)\sin(2\pi f_s t) \end{aligned} \tag{19}$$

where $n_m{}^c(t)$, $n_m{}^s(t)$, $n_s{}^c(t)$, and $n_s{}^s(t)$ are mutually independent stationary zero-mean baseband Gaussian processes satisfying

Authorized licensed use limited to: TOHOKU UNIVERSITY. Downloaded on March 07,2010 at 19:56:16 EST from IEEE Xplore. Restrictions apply.

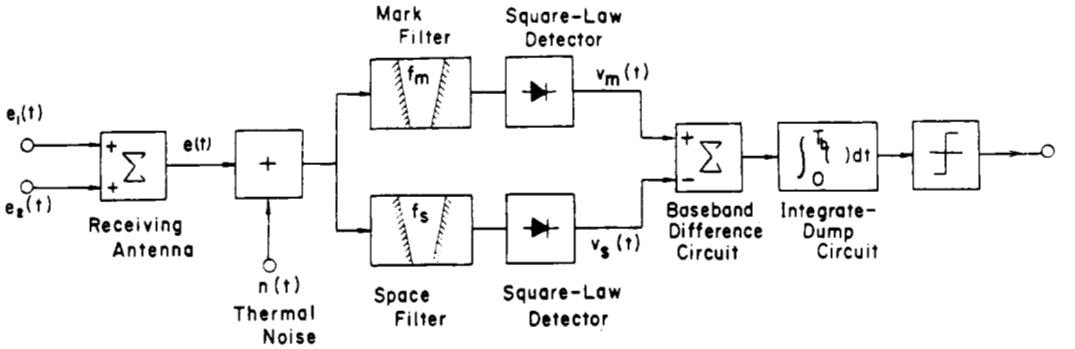

Fig. 3. Block diagram of paging receiver model.

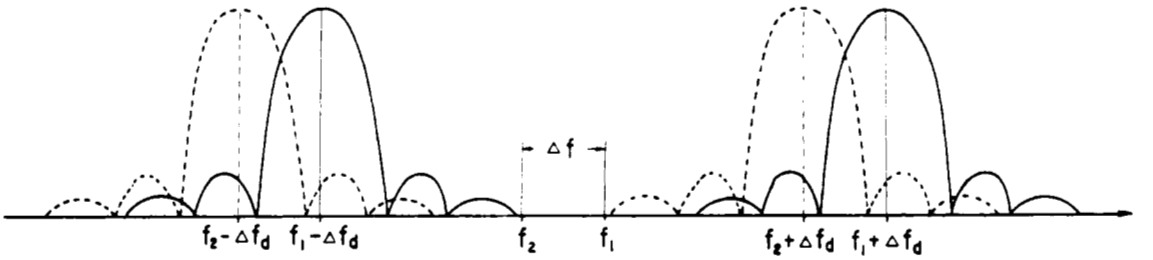

Fig. 4. Power spectrum of combined signal.

the following relations:

$$\langle n_m{}^c(t)\rangle_{\text{av}} = \langle n_m{}^s(t)\rangle_{\text{av}} = \langle n_s{}^c(t)\rangle_{\text{av}} = \langle n_s{}^s(t)\rangle_{\text{av}} = 0$$
$$\langle n_m{}^c(t) n_m{}^c(t \pm \tau)\rangle_{\text{av}} = \langle n_m{}^s(t) n_m{}^s(t \pm \tau)\rangle_{\text{av}} = R_n(\tau)$$
$$\langle n_s{}^c(t) n_s{}^c(t \pm \tau)\rangle_{\text{av}} = \langle n_s{}^s(t) n_s{}^s(t \pm \tau)\rangle_{\text{av}} = R_n(\tau)$$
$$\langle n_m{}^c(t) n_m{}^s(t \pm \tau)\rangle_{\text{av}} = \langle n_m{}^c(t) n_s{}^c(t \pm \tau)\rangle_{\text{av}} = \langle n_m{}^c(t) n_s{}^s(t \pm \tau)\rangle_{\text{av}} = 0$$
$$\langle n_s{}^c(t) n_m{}^s(t \pm \tau)\rangle_{\text{av}} = \langle n_s{}^c(t) n_s{}^s(t \pm \tau)\rangle_{\text{av}} = \langle n_m{}^s(t) n_s{}^s(t \pm \tau)\rangle_{\text{av}} = 0 \tag{20}$$

where $R_n(\tau)$ denotes the covariance function of either bandpass-filtered noise process $n_m(t)$ or $n_s(t)$ and is given by

$$R_n(\tau) = \sigma_n{}^2 \frac{\sin(\pi B\tau)}{(\pi B\tau)} \tag{21}$$

because a bandpass filter with rectangular characteristics is assumed. In (21), $\sigma_n{}^2$ denotes the noise power of the bandpass-filtered noise process and is given by

$$\sigma_n{}^2 = R_n(0) = N_0 B. \tag{22}$$

In the above-described receiver model, errors occur in the following two cases.

Case 1: In spite of the mark signal being sent, the decision of $\epsilon_m < \epsilon_s$ is made.

Case 2: In spite of the space signal being sent, the decision of $\epsilon_m > \epsilon_s$ is made.

In the above situation, ϵ_m and ϵ_s are the time-averaged power values for the two bandpass filter ouptuts and are given by

$$\epsilon_m = \frac{1}{T_b} \int_{-T_b/2}^{T_b/2} \{v_m(t)\}\, dt$$
$$\epsilon_s = \frac{1}{T_b} \int_{-T_b/2}^{T_b/2} \{v_s(t)\}\, dt. \tag{23}$$

Therefore, the error probability P_e can be calculated from

$$P_e = p \cdot \Pr[\epsilon_m < \epsilon_s \mid \text{“}m\text{”}] + (1-p) \cdot \Pr[\epsilon_m > \epsilon_s \mid \text{“}s\text{”}] \tag{24}$$

where p is the probability that mark signal is transmitted. Furthermore, $\Pr[\epsilon_m < \epsilon_s \mid \text{“}m\text{”}]$ and $\Pr[\epsilon_m > \epsilon_s \mid \text{“}s\text{”}]$ denote the probability of occurrence of case 1 and case 2, respectively. Because they are equal to each other, (24) can be represented as

$$P_e = \Pr[\epsilon_m < \epsilon_s \mid \text{“}m\text{”}] = \Pr[\epsilon_m > \epsilon_s \mid \text{“}s\text{”}]. \tag{25}$$

Accordingly, the calculation of error probability P_e is performed assuming that the mark signal is sent. Then, considering that ϵ_m and ϵ_s are given by

$$\epsilon_m = \frac{1}{T_b} \int_{-T_b/2}^{T_b/2} \{e(t) + n_m(t)\}^2\, dt$$
$$\epsilon_s = \frac{1}{T_b} \int_{-T_b/2}^{T_b/2} \{n_s(t)\}^2\, dt \tag{26}$$

and that the three narrow-band Gaussian processes $e(t)$, $n_m(t)$, and $n_s(t)$ are mutually independent, ϵ_m and ϵ_s are mutually

Authorized licensed use limited to: TOHOKU UNIVERSITY. Downloaded on March 07,2010 at 19:56:16 EST from IEEE Xplore. Restrictions apply.

independent random variables. Therefore, the error probability P_e, as represented in (25), can be calculated from

$$P_e = \int_0^\infty \left\{ \int_0^{\epsilon_s} f(\epsilon_m)\, d\epsilon_m \right\} f(\epsilon_s)\, d\epsilon_s \tag{27}$$

where $f(\epsilon_m)$ and $f(\epsilon_s)$ denote the probability density functions of ϵ_m and ϵ_s, respectively. Consequently, it is necessary to calculate $f(\epsilon_m)$ and $f(\epsilon_s)$.

IV. CALCULATION OF $f(\epsilon_m)$ AND $f(\epsilon_s)$

As both random processes $e(t) + n_m(t)$ and $n_S(t)$ are stationary zero-mean narrow-band Gaussian processes with covariance functions $R_s(\tau) + R_n(\tau)$ and $R_n(\tau)$, the problem of calculating $f(\epsilon_m)$ and $f(\epsilon_s)$ can be reduced to the common problem of calculating the probability density function $f(\epsilon_u)$ of a time-averaged power ϵ_u given by

$$\epsilon_u = \frac{1}{T_b} \int_{-T_b/2}^{T_b/2} \{u(t)\}^2\, dt \tag{28}$$

where $u(t)$ is a stationary zero-mean narrow-band Gaussian process represented as

$$u(t) = \xi(t) \cos(2\pi f_0 t) - \eta(t) \sin(2\pi f_0 t) \tag{29}$$

where f_0 is the center frequency corresponding to f_m or f_s and $\xi(t)$ and $\eta(t)$ are mutually independent stationary zero-mean baseband Gaussian processes satisfying the following relations:

$$\begin{aligned} &\langle \xi(t) \rangle_{\text{av}} = \langle \eta(t) \rangle_{\text{av}} = 0 \\ &\langle \xi(t)\xi(t \pm \tau) \rangle_{\text{av}} = \langle \eta(t)\eta(t \pm \tau) \rangle_{\text{av}} = R_u(\tau) \\ &\langle \xi(t)\eta(t \pm \tau) \rangle_{\text{av}} = 0. \end{aligned} \tag{30}$$

In the above equation $R_u(\tau)$ denotes the covariance function of $\xi(t)$ and $\eta(t)$ and is given by

$$R_u(\tau) = \begin{cases} R_s(\tau) + R_n(\tau), & \text{for } u(t) = v_m(t) \\ R_n(\tau), & \text{for } u(t) = v_s(t) \end{cases} \tag{31}$$

where $R_s(\tau)$ and $R_n(\tau)$ are given by (14) and (21), respectively.

Substituting (29) into (28) and neglecting the double frequency term, the time-averaged power ϵ_u is given by

$$\epsilon_u = \frac{1}{T_b} \int_{-T_b/2}^{T_b/2} \{\xi^2(t) + \eta^2(t)\}\, dt. \tag{32}$$

Mutually independent stationary zero-mean baseband Gaussian processes $\xi(t)$ and $\eta(t)$ can be represented by Karhunen–Loeve expansions [5]:

$$\begin{aligned} \xi(t) &= \sum_{\nu=1}^{\infty} \xi_\nu \varphi_\nu(t) \\ \eta(t) &= \sum_{\nu=1}^{\infty} \eta_\nu \varphi_\nu(t) \end{aligned} \tag{33}$$

where $\varphi_\nu(t)$ ($\nu = 1, 2, \cdots$) denotes the orthonormal eigenfunction of the following Fredholm-type integral equation:

$$\lambda_\nu \varphi_\nu(t) = \int_{-T_b/2}^{T_b/2} R_u(t - \tau)\varphi_\nu(\tau)\, d\tau. \tag{34}$$

Furthermore, ξ_ν and η_ν ($\nu = 1, 2, \cdots$) are mutually independent zero-mean Gaussian variables with the variance of λ_ν, where $\lambda_\nu > 0$ is the eigenvalue corresponding to the eigenfunction $\varphi_\nu(t)$.

Substituting (33) into (32) and using the following relation with regard to the orthonormal eigenfunction $\varphi_\nu(t)$,

$$\int_{-T_b/2}^{T_b/2} \varphi_\nu(t)\varphi_\mu(t)\, dt = \begin{cases} 1, & \text{for } \nu = \mu \\ 0, & \text{for } \nu \neq \mu \end{cases} \tag{35}$$

the time-averaged power ϵ_u can be represented as the following truncated series:

$$\epsilon_u = \sum_{\nu=1}^{\infty} \epsilon_{u_\nu} = \frac{1}{2T_b} \sum_{\nu=1}^{\infty} (\xi_\nu{}^2 + \eta_\nu{}^2). \tag{36}$$

As ξ_ν and η_ν are mutually independent zero-mean Gaussian variables with the variance of λ_ν, each ϵ_ν is chi-square distributed with two degrees of freedom. That is, its probability density function $f(\epsilon_{u_\nu})$ is given by

$$f(\epsilon_{u_\nu}) = \begin{cases} \dfrac{1}{(\lambda_\nu/T_b)} \exp\left\{ -\dfrac{\epsilon_{u_\nu}}{(\lambda_\nu/T_b)} \right\}, & \text{for } \epsilon_{u_\nu} \geqslant 0 \\ 0, & \text{for } \epsilon_{u_\nu} < 0. \end{cases} \tag{37}$$

Therefore, the characteristic function $C_{\epsilon_{u_\nu}}(j\omega)$ of ϵ_{u_ν} is given by,

$$\begin{aligned} C_{\epsilon_{u_\nu}}(j\omega) &= \int_{-\infty}^{\infty} f(\epsilon_{u_\nu}) \exp(j\omega\epsilon_{u_\nu})\, d\epsilon_{u_\nu} \\ &= \frac{1}{1 - j\omega(\lambda_\nu/T_b)}. \end{aligned} \tag{38}$$

Because ϵ_u is the total sum of ϵ_{u_ν}, as shown in (36), the characteristic function $C_{\epsilon_u}(j\omega)$ of ϵ_u is given by

$$C_{\epsilon_u}(j\omega) = \prod_{\nu=1}^{\infty} C_{\epsilon_{u_\nu}}(j\omega) = \prod_{\nu=1}^{\infty} \frac{1}{1 - j\omega(\lambda_\nu/T_b)}. \tag{39}$$

Accordingly, $f(\epsilon_u)$ is given by [7]

$$\begin{aligned} f(\epsilon_u) &= \frac{1}{2\pi} \int_{-\infty}^{\infty} C_{\epsilon_u}(j\omega) \exp(-j\omega\epsilon_u)\, d\omega \\ &= \frac{1}{2\pi} \int_{-\infty}^{\infty} \prod_{\nu=1}^{\infty} \frac{\exp(-j\omega\epsilon_u)}{1 - j\omega(\lambda_\nu/T_b)}\, d\omega \\ &= \begin{cases} \displaystyle\sum_{\nu=1}^{\infty} \frac{\exp\{-\epsilon_u/(\lambda_\nu/T_b)\}}{(\lambda_\nu/T_b) \displaystyle\prod_{\substack{\mu=1 \\ \mu\neq\nu}}^{\infty} (1 - \lambda_\mu/\lambda_\nu)}, & \text{for } \epsilon_u \geqslant 0 \\ 0, & \text{for } \epsilon_u < 0. \end{cases} \end{aligned} \tag{40}$$

Authorized licensed use limited to: TOHOKU UNIVERSITY. Downloaded on March 07,2010 at 19:56:16 EST from IEEE Xplore. Restrictions apply.

Thus the problem of calculating $f(\epsilon_m)$ and $f(\epsilon_s)$ can be reduced to the problem of calculating the eigenvalues for the following Fredholm-type integral equations:

$$\lambda_\nu{}^m \varphi_\nu{}^m(t) = \int_{-T_b/2}^{T_b/2} \{R_s(t-\tau)+R_n(t-\tau)\}\varphi_\nu{}^m(\tau)\, d\tau \tag{41}$$

$$\lambda_\nu{}^s \varphi_\nu{}^s(t) = \int_{-T_b/2}^{T_b/2} \{R_n(t-\tau)\}\varphi_\nu{}^s(\tau)\, d\tau. \tag{42}$$

Assuming that both of the received average signal powers $\sigma_1{}^2$ and $\sigma_2{}^2$ are equal to each other, that is,

$$\sigma_1{}^2 = \sigma_2{}^2 = \sigma_s{}^2/2. \tag{43}$$

then the equivalent offset frequencies Δf_1 and Δf_2 given by (12) are

$$\Delta f_1 = \Delta f_2 = \Delta f/2. \tag{44}$$

Therefore, the covariance function $R_s(\tau)$ given by (14) becomes

$$R_s(\tau) = \sigma_s{}^2 \cos(\pi\Delta f\tau) J_0(2\pi f_D \mid \tau \mid). \tag{45}$$

Substituting (45) and (21) into (41) and (42),

$$\lambda_\nu{}^m \varphi_\nu{}^m(t) = \int_{-T_b/2}^{T_b/2} \left[\sigma_s{}^2 \cos\{\pi\Delta f(t-\tau)\} \cdot J_0(2\pi f_D \mid t-\tau \mid) + \sigma_n{}^2 \frac{\sin\{\pi B(t-\tau)\}}{\{\pi B(t-\tau)\}} \right] \varphi_\nu{}^m(\tau)\, d\tau \tag{46}$$

$$\lambda_\nu{}^s \varphi_\nu{}^s(t) = \int_{-T_b/2}^{T_b/2} \left[\sigma_n{}^2 \frac{\sin\{\pi B(t-\tau)\}}{\{\pi B(t-\tau)\}} \right] \varphi_\nu{}^s(\tau)\, d\tau. \tag{47}$$

Denoting α, β, γ, z, and ζ as

$$\alpha = \Delta f T_b, \qquad \beta = f_D T_b, \qquad \gamma = B T_b,$$
$$z = t/T_b, \qquad \zeta = \tau/T_b, \tag{48}$$

(46) and (47) are represented in the normalized form:

$$\lambda_\nu{}^m \varphi_\nu{}^m(z) = \int_{-1/2}^{1/2} \left[\sigma_s{}^2 \cos\{\pi\alpha(z-\zeta)\} J_0(2\pi\beta \mid z-\zeta \mid) + \sigma_n{}^2 \frac{\sin\{\pi\gamma(z-\zeta)\}}{\{\pi\gamma(z-\zeta)\}} \right] \varphi_\nu{}^m(\zeta)\, d\zeta \tag{49}$$

$$\lambda_\nu{}^s \varphi_\nu{}^s(z) = \int_{-1/2}^{1/2} \left[\sigma_n{}^2 \frac{\sin\{\pi\gamma(z-\zeta)\}}{\{\pi\gamma(z-\zeta)\}} \right] \varphi_\nu{}^s(\zeta)\, d\zeta. \tag{50}$$

Assuming that the average signal power of the combined input is much higher than the noise power, that is, $\sigma_s{}^2 \gg \sigma_n{}^2$, (49) is approximately given by

$$\lambda_\nu{}^m \varphi_\nu{}^m(z) \approx \int_{-1/2}^{1/2} [\sigma_s{}^2 \cos\{\pi\alpha(z-\zeta)\} \cdot J_0(2\pi\beta \mid z-\zeta \mid)] \varphi_\nu{}^m(\zeta)\, d\zeta. \tag{51}$$

Furthermore, assuming that the maximum Doppler shift frequency is much lower than the signaling frequency, that is, $\beta = f_D T_b \ll 1$, the Bessel function included in the bracket of (51) can be approximated as

$$J_0(2\pi\beta \mid z-\zeta \mid) \approx 1, \qquad \text{for } -\tfrac{1}{2} \leqslant z, \quad \zeta \leqslant \tfrac{1}{2}. \tag{52}$$

Therefore, (51) can be represented as

$$\lambda_\nu{}^m \varphi_\nu{}^m(z) \approx \int_{-1/2}^{1/2} [\sigma_s{}^2 \cos\{\pi\alpha(z-\zeta)\}] \varphi_\nu{}^m(\zeta)\, d\zeta. \tag{53}$$

Eigenvalues $\lambda_\nu{}^m$ for this integral equation can easily be solved in the closed form

$$\lambda_1{}^m = \tfrac{1}{2}(\sigma_s{}^2 T_b)\left\{1 + \frac{\sin(\pi\alpha)}{(\pi\alpha)}\right\}$$
$$\lambda_2{}^m = \tfrac{1}{2}(\sigma_s{}^2 T_b)\left\{1 - \frac{\sin(\pi\alpha)}{(\pi\alpha)}\right\}$$
$$\lambda_3{}^m = \lambda_4{}^m = \cdots = 0. \tag{54}$$

Eigenvalues $\lambda_\nu{}^s$ for (50) have already been solved by Slepian, Pollak, and Landau [7]–[10] and are given by

$$\lambda_\nu{}^s = (\sigma_n{}^2 T_b)\gamma \left\{ R_{0\nu}{}^{(1)}\left(\frac{\pi}{2}\gamma, 1\right)\right\}^2 \cdots (\nu = 1, 2, 3, \cdots) \tag{55}$$

where $R_{0\nu}{}^{(1)}(c, x)$ denotes prolate spheroidal wave function of the first kind. Considering that the bandwidth B of each bandpass filter is set as in (18), the parameter γ, included in (55), is given by

$$\gamma = 2 + \alpha. \tag{56}$$

Therefore, (55) is rewritten as

$$\lambda_\nu{}^s = (\sigma_n{}^2 T_b)(2+\alpha)\left\{ R_{0\nu}{}^{(1)}\left(\frac{\pi}{2}(2+\alpha), 1\right)\right\}^2 \cdots (\nu = 1, 2, 3, \cdots). \tag{57}$$

Using (40), (54), and (57), the probability density functions

Authorized licensed use limited to: TOHOKU UNIVERSITY. Downloaded on March 07,2010 at 19:56:16 EST from IEEE Xplore. Restrictions apply.

$f(\epsilon_m)$ and $f(\epsilon_s)$ are given, respectively, by

$$f(\epsilon_m) = \begin{cases} \dfrac{\pi\alpha}{\sigma_s^2 \sin(\pi\alpha)} \left[\exp\left(-2\epsilon_m \Big/ \sigma_s^2 \left\{1 + \dfrac{\sin(\pi\alpha)}{\pi\alpha}\right\}\right) \right. \\ \quad \left. - \exp\left(-2\epsilon_m \Big/ \sigma_s^2 \left\{1 - \dfrac{\sin(\pi\alpha)}{\pi\alpha}\right\}\right)\right], \\ \qquad \text{for } \epsilon_m \geqslant 0 \\ 0, \quad \text{for } \epsilon_m < 0 \end{cases} \tag{58}$$

$$f(\epsilon_s) = \begin{cases} \displaystyle\sum_{\nu=1}^{\infty} \frac{\exp\{-\epsilon_s/\sigma_n^2 A_\nu(a)\}}{\sigma_n^2 A_\nu(\alpha) \prod_{\substack{\mu=1 \\ \mu\neq\nu}}^{\infty} [1 - \{A_\mu(\alpha)/A_\nu(\alpha)\}]}, \\ \qquad \text{for } \epsilon_s \geqslant 0, \\ 0, \quad \text{for } \epsilon_s < 0, \end{cases} \tag{59}$$

where $A_\nu(\alpha)$ is given by

$$A_\nu(\alpha) = (2+\alpha)\left\{R_{0\nu}^{(1)}\left(\frac{\pi}{2}(2+\alpha), 1\right)\right\}^2 \quad \cdots (\nu = 1, 2, 3, \cdots). \tag{60}$$

Using (58) and (59), $f(\epsilon_m)$ and $f(\epsilon_s)$, when the normalized offset frequency α is a parameter, can be calculated as shown in Figs. 5 and 6.

V. CALCULATION OF THE ERROR PROBABILITY

Substituting (58) and (59) into (27), the error probability P_e can be represented as

$$P_e = \int_0^\infty F(\epsilon_s) \cdot \left\{ \sum_{\nu=1}^{\infty} \frac{\exp\{-\epsilon_s/\sigma_n^2 A_\nu(\alpha)\}}{\sigma_n^2 A_\nu(\alpha) \prod_{\substack{\mu=1 \\ \mu\neq\nu}}^{\infty} [1 - \{A_\mu(\alpha)/A_\nu(\alpha)\}]} \right\} d\epsilon_s \tag{61}$$

where $F(\epsilon_s)$ is given by

$$\begin{aligned} F(\epsilon_s) &= \int_0^{\epsilon_s} f(\epsilon_m)\, d\epsilon_m \\ &= 1 - \frac{1}{2}\left[\left\{\frac{\pi\alpha}{\sin(\pi\alpha)} + 1\right\} \cdot \exp\left(-2\epsilon_s \Big/ \sigma_s^2 \left\{1 + \frac{\sin(\pi\alpha)}{\pi\alpha}\right\}\right) \right. \\ &\quad \left. - \left\{\frac{\pi\alpha}{\sin(\pi\alpha)} - 1\right\} \exp\left(-2\epsilon_s \Big/ \sigma_s^2 \left\{1 - \frac{\sin(\pi\alpha)}{\pi\alpha}\right\}\right)\right]. \end{aligned} \tag{62}$$

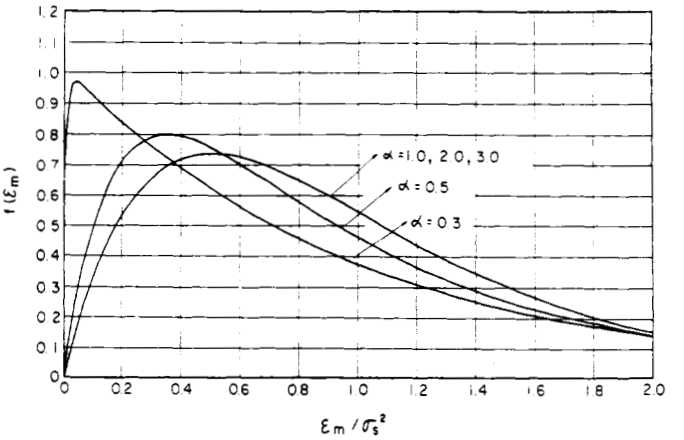

Fig. 5. Probability density function of ϵ_m.

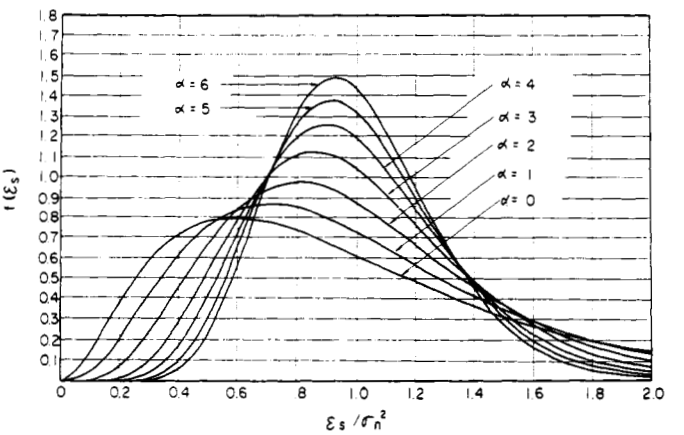

Fig. 6. Probability density function of ϵ_s.

Interchanging the integration and summation functions, (61) can be rewritten as

$$Pe = \sum_{\nu=1}^{\infty} \frac{1}{\sigma_n^2 A_\nu(\alpha) \prod_{\substack{\mu=1 \\ \mu\neq\nu}}^{\infty} [1 - \{A_\mu(\alpha)/A_\nu(\alpha)\}]} \cdot \int_0^\infty F(\epsilon_s) \exp\{-\epsilon_s/\sigma_n^2 A_\nu(\alpha)\}\, d\epsilon_s. \tag{63}$$

Therefore, the error probability P_e is given by

$$P_e = \sum_{\nu=1}^{\infty} \frac{1}{\prod_{\substack{\mu=1 \\ \mu\neq\nu}}^{\infty} [1 - \{A_\mu(\alpha)/A_\nu(\alpha)\}]} \cdot \frac{4\{A_\nu(\alpha)\}^2}{\left(\dfrac{\sigma_s^2}{\sigma_n^2}\right)^2 \left\{1 - \dfrac{\sin^2(\pi\alpha)}{(\pi\alpha)^2}\right\} + 4\left(\dfrac{\sigma_s^2}{\sigma_n^2}\right) A_\nu(\alpha) + \{4 A_\nu(\alpha)\}^2}. \tag{64}$$

Using (64), the variation of P_e versus signal energy to noise power density ratio ϵ_b/N_0, which is denoted by

$$\epsilon_b/N_0 = (\sigma_s^2 T_b)/N_0 = (\sigma_s^2 \sigma_n^2) \cdot (2+\alpha), \tag{65}$$

Authorized licensed use limited to: TOHOKU UNIVERSITY. Downloaded on March 07,2010 at 19:56:16 EST from IEEE Xplore. Restrictions apply.

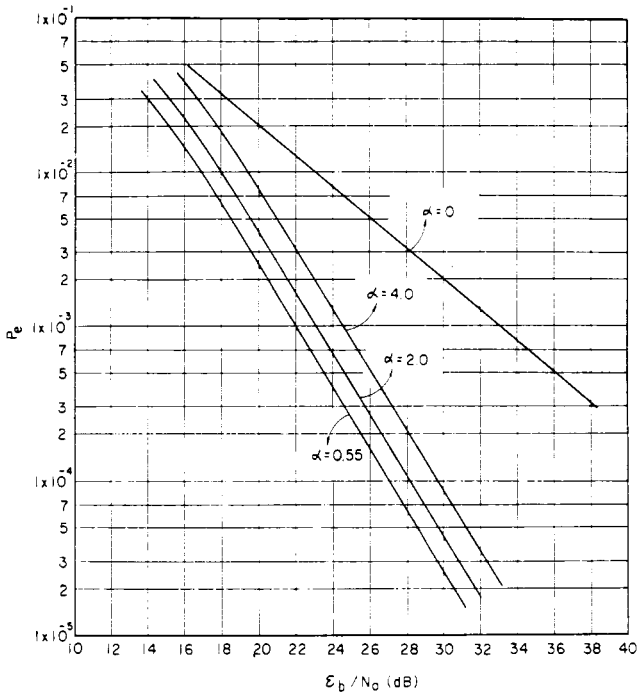

Fig. 7. Error rate performance with offset frequency as a parameter.

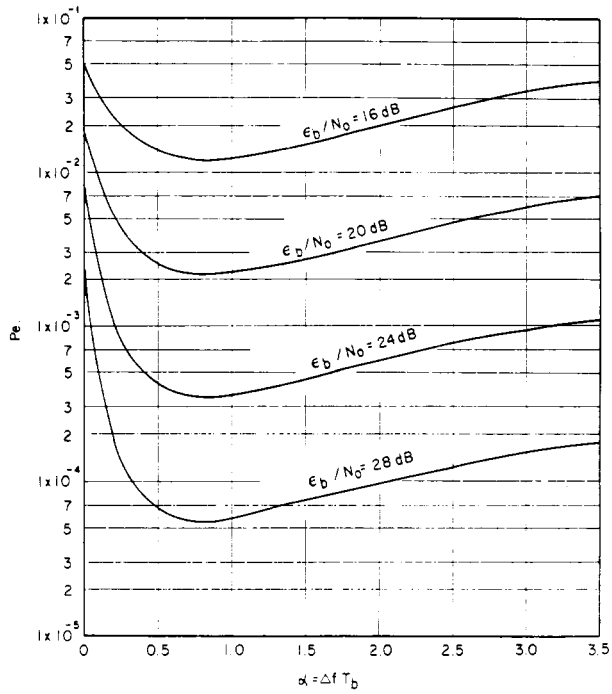

Fig. 8. Error rate versus offset frequency.

can be calculated, as shown in Fig. 7. Furthermore, the variation of P_e versus α can also be calculated, as shown in Fig. 8. From those results, the following concluding remarks are obtained.

1) An optimum value exists in normalized offset frequency $\alpha = \Delta f T_b$ which minimizes the error probability P_e.
2) The optimum value of $\alpha \approx 0.55$ is not closely dependent on the signal energy to noise power density ratio ϵ_b/N_0.
3) Unless the normalized offset frequency is out of the range $0.5 < \alpha < 1.5$, the error rate performance degrades little from the optimum performance.
4) In case of the optimum setting, the improvement effect for ϵ_b/N_0 is about 10 dB for the error probability of $P_e = 1 \times 10^{-3}$, when compared with the case of $\alpha = 0$. The physical meaning of this improvement effect will be explained in the following section.

VI. PHYSICAL MEANING OF THE IMPROVEMENT

Let us consider the case wherein the offset frequency Δf is much lower than the signaling frequency $f_b = 1/T_b$, that is, $\alpha = \Delta f T_b \ll 1$. In this case the combined input signal $e(t)$ given by (7) can be regarded of nearly constant value during a time slot T_b, because the multipath fading phenomenon, which occurred on $e(t)$, is assumed to be quasistationary Rayleigh fading. That is, the maximum Doppler shift frequency f_D is also much smaller than f_b. Then, the envelope of $e(t)$ during a time slot becomes a Rayleigh distributed random variable. Therefore, if the signal power σ_s^2 is much larger than the noise power σ_n^2, that is, $\sigma_s^2 \gg \sigma_n^2$, the time-averaged power ϵ_m given by (26) becomes a random variable, which follows an exponential distribution law. This is proved by the curve of $\alpha = 0$ in Fig. 5. Considering that the error rate performance is closely dependent on the probability distribution of ϵ_m, it is reasonable that the curve of $\alpha = 0$ in Fig. 7 be nearly equal to the well-known error rate performance for an FSK system using an energy detection scheme in the quasi-stationary Rayleigh fading environment.

Letting the offset frequency be increased from the above case, the combined input signal $e(t)$ during a time slot T_b cannot be regarded as a constant value. Therefore, the time-averaged power ϵ_m becomes a random variable, which follows a different distribution law from an exponential law. As shown in Fig. 5, the probability distribution of ϵ_m becomes a sharper distribution with small variance, such as the Gamma distribution. This means that the fading dynamic range of ϵ_m is reduced by the averaging effect. On the other hand, the probability distribution of ϵ_s does not vary from that of the quasi-stationary case. Therefore, the error rate performance can be improved by increasing the offset frequency.

When the offset frequency is excessively increased, that is, $\alpha = \Delta f T_b > 2$, the probability distribution of ϵ_m varies little from the above sharper distribution. However, that of ϵ_s becomes a broader distribution with large variance, compared with the above two cases, because the bandwidth B of the two bandpass filters given by (18) is widened for distortionless reception. Therefore, the improvement effect is reduced. It has already been shown that the same improvement effect also occurs in an FSK system using an energy detection scheme in a fast Rayleigh fading environment [11].

VII. CONCLUSION

An improvement effect occurring in a multistation digital radio paging system, using an FSK with energy detection scheme and a carrier frequency offset strategy, has been theoretically analyzed. The improvement effect is caused by the fact that the probability distribution of the time-averaged signal power is

Authorized licensed use limited to: TOHOKU UNIVERSITY. Downloaded on March 07,2010 at 19:56:16 EST from IEEE Xplore. Restrictions apply.

transformed in company with the increase in offset frequency. However, if the offset frequency is excessively increased, the noise power is increased, because the bandpass filter bandwidth must be widened. Therefore, the offset frequency must be set equal to an optimum value.

ACKNOWLEDGMENT

The authors wish to thank S. Itoh and M. Kohmuara for their helpful guidance. They also wish to thank Dr. H. Miyakawa and Dr. H. Harashima for their helpful discussions.

REFERENCES

[1] G. D. Gray, "The simulcasting techniques: An approach to total-area radio coverage," *IEEE Trans. Veh. Technol.*, vol. VT-28, pp. 117–125, May 1979.

[2] T. Hattori and K. Hirade, "Multitransmitter digital signal transmission by using offset frequency strategy in a land-mobile telephone system," *IEEE Trans. Veh.Technol.*, vol. VT-27, pp. 231–238, Nov. 1978.

[3] M. Komura *et al.*, "New radio paging system and its propagation charcteristics," *IEEE Trans. Veh. Technol.*, vol. VT-26, pp. 362–366, Nov. 1977.

[4] M. J. Gans, "A power-spectral theory of propagation in the mobile radio environment," *IEEE Trans. Veh. Technol.*, vol. VT-21, pp. 27–38, Feb. 1972.

[5] W. B. Davenport, Jr., and W. L. Root, *Introduction to Random Signals and Noise*. New York: McGraw-Hill, 1958, pp. 96–98.

[6] *ibid.*, pp. 193–199.

[7] D. Slepian and H. O. Pollak, "Prolate spheroidal wave functions, Fourier analysis and uncertainty—I," *Bell Syst. Tech. J.*, vol. 40, pp. 43–63, Jan. 1961.

[8] H. J. Landau and H. O. Pollak, "Prolate spheroidal wave functions, Fourier analysis and uncertainty—II," *Bell Syst. Tech. J.*, vol. 40, pp. 65–84, Jan. 1961.

[9] ——, "Prolate spheroidal wave functions, Fourier analysis and uncertainty—III: Time dimension of the space of essentially time and band limited signals," *Bell Syst. Tech. J.*, vol. 41, pp. 1295–1336, July 1962.

[10] D. Slepian and E. Sonnenblick, "Eigenvalues associated with prolate spheroidal wave functions of zero order," *Bell Syst. Tech. J.* vol. 44, pp. 1745–1759, Oct. 1965.

[11] I. Jacobs, "Energy detection of Gaussian communication signals," in *Proc. IEEE 10th Nat. Commun. Symp.*, pp. 440–448, Oct. 1964.

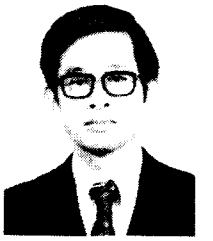

Takeshi Hattori (M'74) was born in Mie, Japan, on August 6, 1945. He received the B.S.E.E., M.S.E.E., and D.S.E.E. degrees from Tokyo University, Tokyo, in 1969, 1971, and 1974, respectively.

Since 1974 he has been with the Electrical Communication Laboratories, Nippon Telegraph and Telephone Public Corporation, and has been engaged in the research of multitransmitter simulcasting techniques in the digital mobile radio communications, fading, and impulsive noise simulators for V/UHF land mobile radio, compandor for improving the speech quality of the 800-MHz mobile telephone system, and so on. He is now a Staff Engineer of the Mobile Communication Systems Section of the Integrated Transmission Systems Development Division of NTT.

Dr. Hattori is a member of the Institute of Electronics and Communications Engineers of Japan and the IEEE Vehicular Techology Society.

Kenkichi Hirade (M'79) was born in Nagoya, Japan, on August 25, 1942. He received the B.S.E.E. and M.S.E.E. degrees from Nagoya University, Nagoya, in 1965 and 1967, respectively.

Since 1967 he has been with the Electrical Communication Laboratories, Nippon Telegraph and Telephone Public Corporation. From 1967 to 1973 he was engaged in the research of a clock synchronizer for the PCM-TDMA satellite communication system and carrier synchronizer for the quasi-millimeter digital radio relay system. Since 1973 he has been engaged in the research of digital mobile radio communication systems.

Mr. Hirade is a member of the Institute of Electronics and Communications Engineers of Japan.

Fumiyuki Adachi (M'79) was born in Niigata, Japan, on April 24, 1950. He received the B.S.E.E. degree from Tohoku University, Sendai, in 1973.

Since 1973 he has been with the Electrical Communication Laboratories, Nippon Telegraph and Telephone Public Corporation. From 1973 to 1978 he was engaged in the research of diversity techniques for mobile radio communication systems. Since 1979 he has been engaged in the research of mobile radio control systems.

Mr. Adachi is a member of the Institute of Electronics and Communication Engineers of Japan.

Authorized licensed use limited to: TOHOKU UNIVERSITY. Downloaded on March 07,2010 at 19:56:16 EST from IEEE Xplore. Restrictions apply.